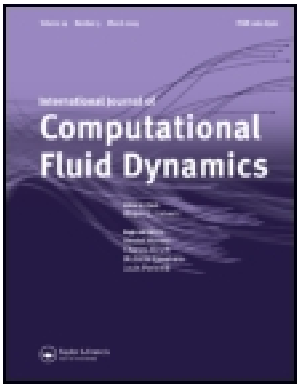

International Journal of Computational Fluid Dynamics
Publication details, including instructions for authors and subscription information:
http://www.tandfonline.com/loi/gcfd20

Dynamics of the blood flow in the curved artery with the rolling massage

H.H. Yi [a] , X.H. Wu [a] & Y.L. Yao [a]

[a] Department of Physics and Electronics Science, Institute of Theoretical Physics, Binzhou University, Shandong, 256603, China

Available online: 21 Nov 2011

International Journal of Computational Fluid Dynamics
Vol. 25, No. 9, October–November 2011, 501–507

Dynamics of the blood flow in the curved artery with the rolling massage

H.H. Yi*, X.H. Wu and Y.L. Yao

Department of Physics and Electronics Science, Institute of Theoretical Physics, Binzhou University, Shandong 256603, China

(*Received 20 May 2011; final version received 9 October 2011*)

Arterial wall shear stress and flow velocity are important factors in the development of some arterial diseases. Here, we aim to investigate the dynamic effect of the rolling massage on the property of the blood flow in the curved artery. The distributions of flow velocity and shear stress for the blood flow are computed by the lattice Boltzmann method, and the dynamic factors under different rolling techniques are studied numerically. The study is helpful to understand the mechanism of the massage and develop the massage techniques.

Keywords: lattice Boltzmann method; rolling massage; blood flow; arterial diseases; rolling techniques

1. Introduction

Arterial diseases are some of the most life-threatening diseases. The blood flow, especially at the bending and bifurcation of the arteries, is an important topic in the study of haemodynamics. There is evidence that suggests a correlation between the arterial diseases and regions of low blood-flow velocity, rotational flow, high particle residence time and low and oscillatory shear stress near the walls of the arteries. Studying the blood flows and the haemodynamic factors in the bending artery is of great importance in medical science (Fung 1997) and is currently receiving more and more attention.

Chinese Medical Massage (CMM, also called tui na in China) is one branch of Chinese Medicine. Due to its agile usage, simple manner, safety and practicality, it is referred to as 'Green Treatment' in eliminating various diseases (Maria 1997). As a natural therapy, massage is a method used to relieve muscle stiffness, remove blockages and promote blood circulation by the rubbing, kneading, pressing, nipping and twisting of parts of the body. Although this technique has been used in the Orient for centuries, the mechanism is far from being understood. In order to understand the mechanism of massage in promoting blood circulation, we have investigated the effect of rolling massage on the behaviour of the blood flows in the artery numerically and found that suitable massage technique can aid blood circulation (Yi *et al*. 2005, Yi 2010).

The lattice Boltzmann method (LBM; Benzi *et al*. 1992, Chen *et al*. 1992, Chen and Doolen 1998, Qian *et al*. 1992) has been recognised as an alternate method in computational fluid dynamics since its proposal. Recently, the LBM has been successfully extended to simulate the blood flow, including transient blood flow passing through an artificial aortic valve (Krafczyk *et al*. 1998), unsteady and pulsatile blood flow in distensible blood vessels (Fang *et al*. 2002, Hoekstra *et al*. 2003, Boyd *et al*. 2004), single leukocyte rolling (Migliorini *et al*. 2002, Sun *et al*. 2003), transporting of particles in symmetric severely stenotic arteries (Li *et al*. 2004a), erythrocyte deformation (Li *et al*. 2008), blood cell dynamics (Dupin *et al*. 2008) and multi-component blood flow (Dupin *et al*. 2003). Many studies concentrate on the behaviour of the blood flow in the region where the arterial diseases are prone to develop. Artoli *et al*. (2004) simulate steady flow in two-dimensional symmetric bifurcation. The blood flow in a two-dimensional model of optimum bifurcation geometry is investigated in order to explain the haemodynamic mechanism of the predilection of the atherosclerotic lesions at these sites (Ji *et al*. 2009, 2010). Boyd *et al*. (2005) simulate the flow velocity and shear stress in a two-dimensional carotid artery with stenosis growth and further investigate how the velocity and shear vary between Newtonian and non-Newtonian flows (Boyd and Buick 2007). The flow mechanism in curved pipe is also investigated by Boyd *et al*. (2007) and Kang *et al*. (2008) in two and three dimensions, respectively.

The distributions of dynamic factors are important factors in the development of some arterial diseases. The numerical simulations and flow visualisations of blood flow are of great significance in the study of the haemodynamics. This paper focuses on the investigation of the property of the blood flow in the bending

*Corresponding author. Email: houhuily@163.com

ISSN 1061-8562 print/ISSN 1029-0257 online

http://dx.doi.org/10.1080/10618562.2011.632373
http://www.tandfonline.com

artery. The distributions of velocity and shear stress in the bend under rolling manipulation are obtained. The effect of rolling technique factors, including the rolling velocity and rolling protuberance length, on the near-wall shear stress is computed in the bending artery.

2. The lattice Boltzmann model

We choose to work on a two-dimensional square lattice with nine velocities. Let $f_i(\mathbf{x},t)$ be a non-negative real number describing the distribution function of the fluid density at site $\mathbf{x}$ at time t moving in direction $\mathbf{e}_i$. Here, $\mathbf{e}_0 = (0,0)$, $\mathbf{e}_i = (\cos \pi(i-1)/2, \sin \pi(i-1)/2)$, for $i = 1, 2, 3, 4$, and $\mathbf{e}_i = \sqrt{2}(\cos \pi(2i-1)/4, \sin \pi(2i-1)/4)$, for $i = 5, 6, 7, 8$, are the nine possible velocity vectors. The distribution functions evolve according to a Boltzmann equation that is discrete in both space and time (Qian *et al.* 1992):

$$f_i(\mathbf{x} + \mathbf{e}_i, t+1) - f_i(\mathbf{x}, t) = -\frac{1}{\tau}(f_i - f_i^{\mathrm{eq}}). \quad (1)$$

The density ρ and macroscopic velocity $\mathbf{u}$ are defined by

$$\rho = \sum_i f_i, \quad \rho\mathbf{u} = \sum_i f_i \mathbf{e}_i, \quad (2)$$

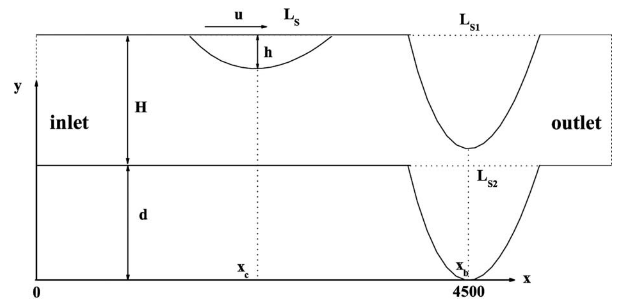

Figure 1. Schematic diagram of a curved artery with the rolling massage manipulation on the upper boundary in two dimensions.

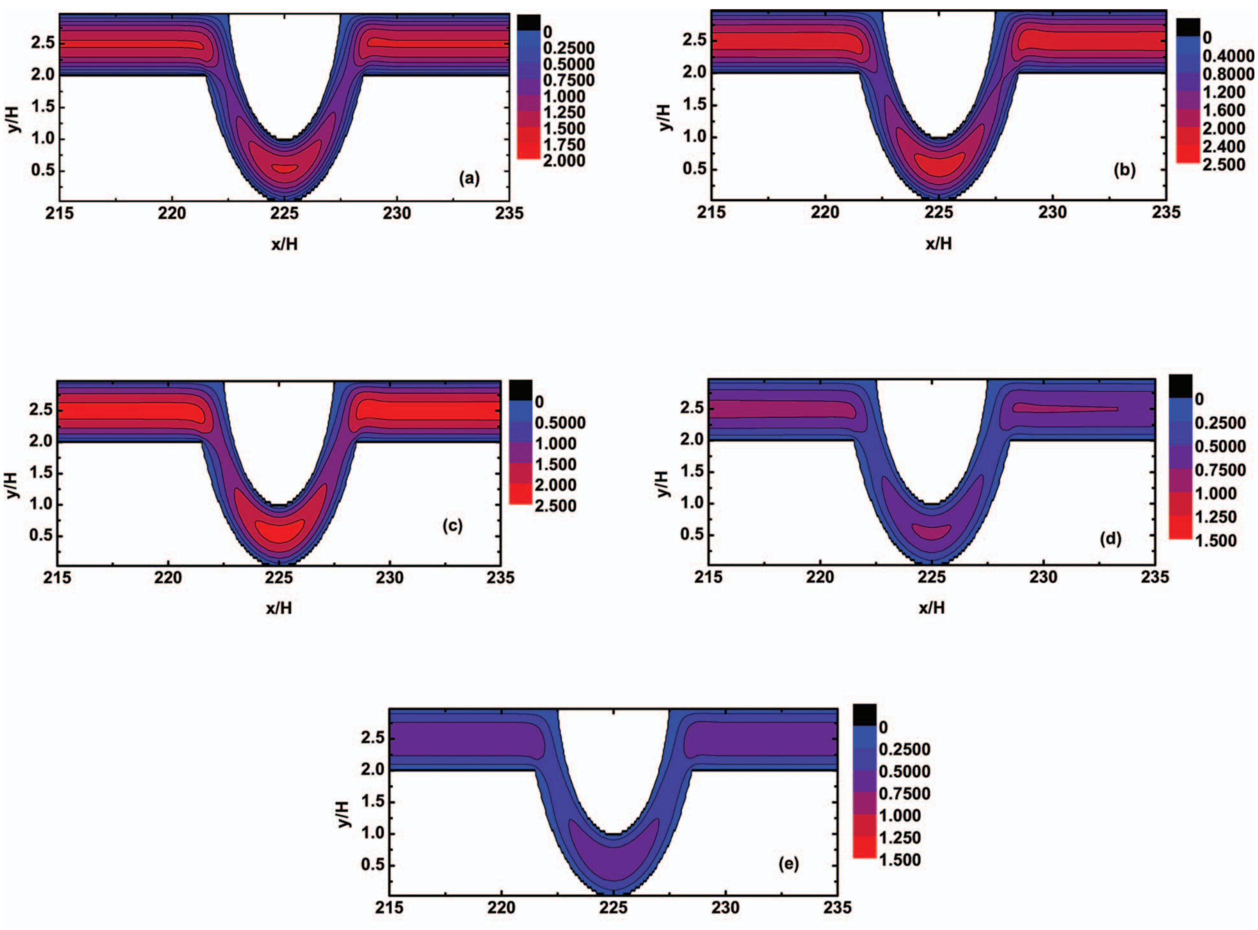

Figure 2. The distributions of the relative flow velocity v/u_0 at the bending artery at some typical times. Before beginning rolling massage (a) and at rolling massage time $T/4$ (b), $T/2$ (c), $3T/4$ (d) and T (e). The relative rolling velocity is 3.74, the maximal relative rolling depth h_m/H is 0.6 and the length of the protuberance L_s is 300.

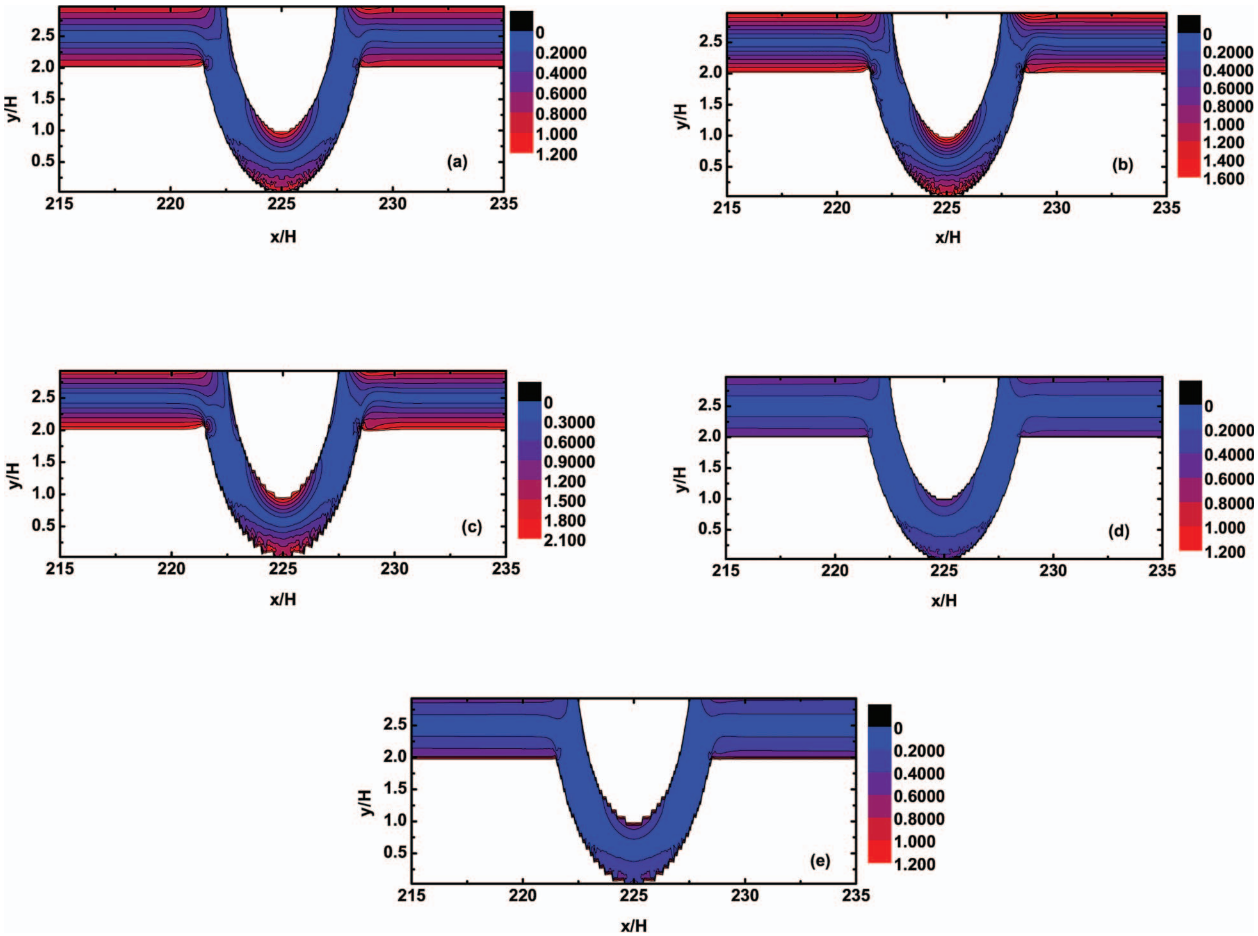

Figure 3. The contour of the relative shear stress σ/σ_n at the bending artery at some typical times. Before beginning rolling massage (a) and at rolling massage time $T/4$ (b), $T/2$ (c), $3T/4$ (d) and T (e). The relative rolling velocity is 3.74, the maximal relative rolling depth h_m/H is 0.6 and the length of the protuberance L_s is 300.

and the equilibrium distribution functions f_i^{eq} are usually supposed to be dependent only on the local density ρ and flow velocity $\mathbf{u}$. A suitable choice reads

$$f_i^{eq} = \rho\alpha_i\left[1 + 3\mathbf{e}_i \cdot \mathbf{u} + \frac{9}{2}(\mathbf{e}_i \cdot \mathbf{u})^2 - \frac{3}{2}u^2\right], \qquad (3)$$

where $\alpha_0 = 4/9$, $\alpha_1 = \alpha_2 = \alpha_3 = \alpha_4 = 1/9$ and $\alpha_5 = \alpha_6 = \alpha_7 = \alpha_8 = 1/36$. The macroscopic equations can be obtained by a Chapman–Enskog procedure. The pressure and the kinematic viscosity is defined by the equations $p = c_s^2\rho$ with $c_s^2 = 1/3$ and $v = (2\tau - 1)/6$, respectively.

3. Results and discussion

In this study, we consider a simplified model of a two-dimensional bending artery as illustrated in Figure 1. The blood vessel is a long and thin tube with a fraction of arc-shaped bending artery. The bending part's x-directional position x_b is 4500. The entrance and exit of the bend's x-directional position are 4430 and 4570, respectively. The length L and diameter H of the blood vessel are 5200 and 20, respectively, in lattice unit. The bending lengths L_{s1} on the upper boundary and L_{s2} on the lower boundary are 100 and 140, respectively, and the bending depth d of each boundary is 40 in lattice unit. An arc-shaped protuberance moves with a velocity u from $x_c = 600$ to $x_c = 1600$ on the upper boundary due to rolling massage manipulation, and the rolling time in this process is denoted by T. The length of the protuberance (also called the rolling protuberance length) is denoted by L_s. The thickness of the protuberance is h, which is the rolling massage depth. The radius of the arc is $r = h/2 + L_s^2/8h$. Here, h is assumed to vary with respect to time t as

$$h = \begin{cases} h_m t/T & 0 \le t < \frac{T}{2} \\ h_m(1 - t/T) & \frac{T}{2} \le t < T, \end{cases} \tag{4}$$

where h_m is the maximal rolling massage depth. The maximal relative rolling massage depth is defined as h_m/H. The rolling velocity to the blood velocity (relative rolling velocity) is u/u_0, where u_0 is the average blood velocity at inlet (outlet) of the vessel in the case of without rolling manipulation. The Reynolds number *Re* is defined as u_0H/ν.

In the study, the blood flow is assumed to have a mass density of 1 in lattice unit; $\tau = 0.517$ in each simulation. The pressure drop between inlet and outlet is set to be 0.006. Initially, the distribution functions at all the fluid nodes are set to be the equilibrium distribution functions with zero velocity except for those at inlet and outlet. The rolling massage manipulation is exerted after the first 100,000 time steps. The boundary condition for the moving stenosis is treated by the method proposed in Li *et al.* (2004b). Pressure boundary condition is implemented at the inlet and outlet (Zou and He 1997). The shear stress is calculated by the method depicted by Inamuro *et al.* (2000). The Reynolds number *Re* is 7.87 in each simulation.

3.1. The blood flow in the bending artery under rolling manipulation

Figures 2(a) and 3(a) show the distribution of the relative flow velocity v/u_0 and relative shear stress σ/σ_n at bending artery in the case of without rolling massage; σ_n is 5.17×10^{-6} in lattice unit, which denotes the near-wall shear stress at $x/H = 215$. At the region near the entrance (exit) of the bending artery, the upper boundary acts as the outer bend, and, consequently, the lower boundary acts as the inner bend. However, at the region near the bottom of the bending artery, the upper boundary acts as the inner bend. The flow near the inner bend is larger than that near the outer bend as displayed in Figure 4 (solid line). At the region after the entrance of the bend and before the exit of the bend, the shear stress is obviously smaller than that of planar channel. The low shear stress contributes to intimal thickening and atherosclerosis development as a local mechanism of the carotid artery in hypertensive patients. The bending artery has large probability in developing atherosclerosis than that in straight part

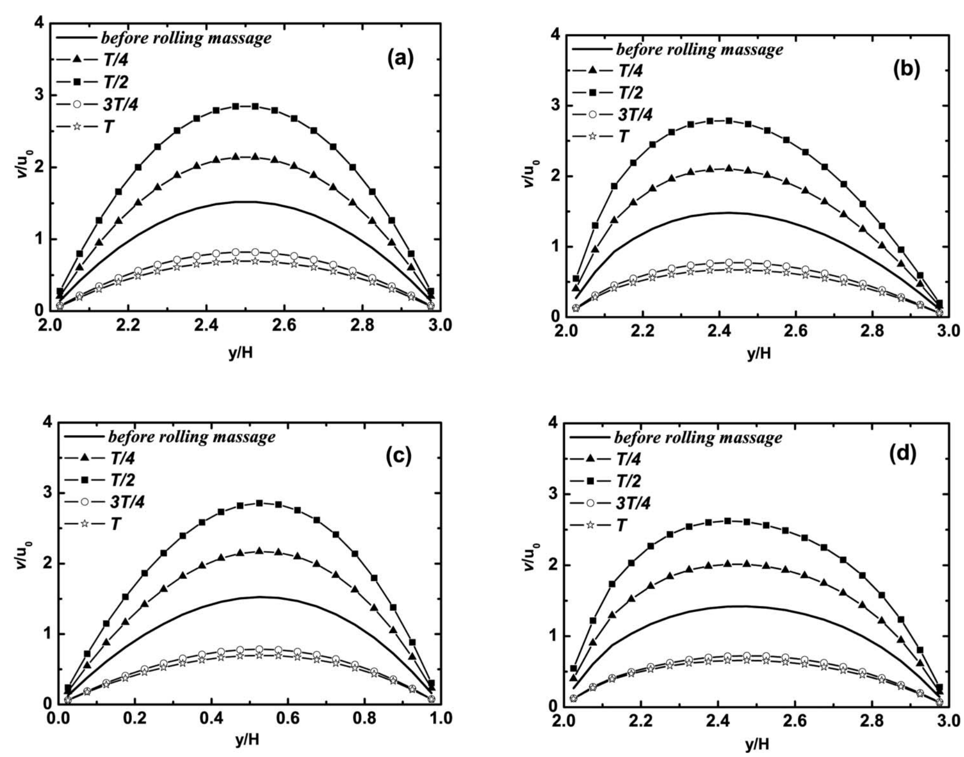

Figure 4. The relative flow velocity v/u_0 at $x/H = 215$ (straight channel; a), $x/H = 221.5$ (entrance of the bend; b), $x/H = 225$ (middle of the bend; c) and $x/H = 228.5$ (exit of the bend; d) in the artery at some typical times. The relative rolling velocity is 3.74, the maximal relative rolling depth h_m/H is 0.6 and the length of the protuberance L_s is 300.

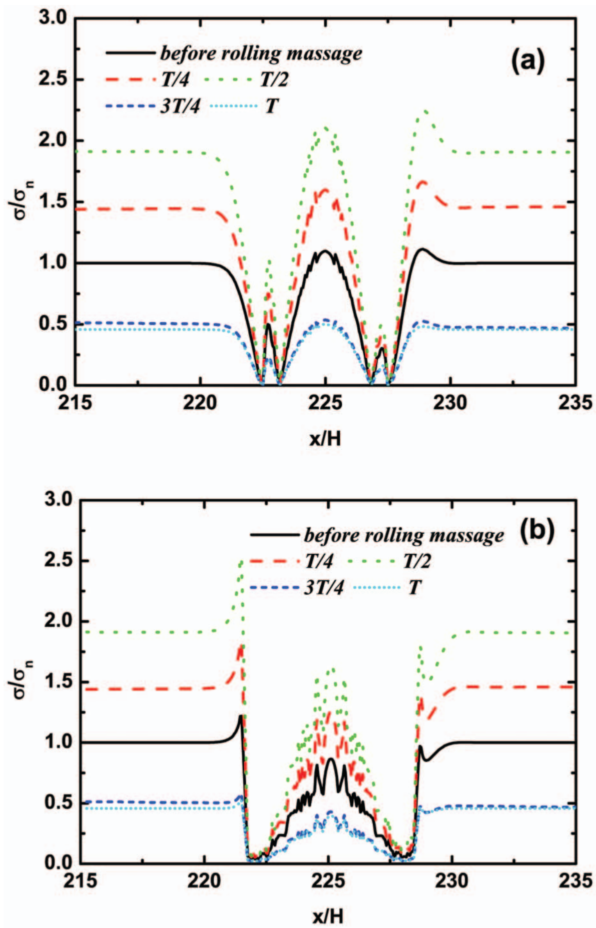

Figure 5. The relative near-wall shear stress $\sigma/\sigma_{\mathrm{n}}$ at the upper boundary (a) and the lower boundary (b) near the bending artery at some typical times. The relative rolling velocity is 3.74, the maximal relative rolling depth h_{m}/H is 0.6 and the length of the protuberance L_{s} is 300.

artery, which is consistent with the clinical observation (McDonald 1974, Fung 1997).

Figures 2 and 3 show the variation of the contour of the flow velocity and shear stress for the relative rolling velocity 3.74 and rolling depth 0.6 at some typical times. The flow velocity and shear stress are greater at $T/4$ and $T/2$, while it is smaller at $3T/4$ and T than that of the normal condition, which is similar to that of the flow at the outlet of the planar channel (Yi *et al.* 2005). The relative flow velocity v/u_0 at entrance (b), middle (c) and exit (d) of the bend at some typical times is also displayed in Figure 4. The relative near-wall shear stress $\sigma/\sigma_{\mathrm{n}}$ at both boundaries of the blood vessel under rolling manipulation at some typical rolling times is also displayed in Figure 5. At $T/4$ and $T/2$, the enhancement of the near-wall shear stress is considerable, which may be helpful for preventing blood particle deposit on the vessel wall.

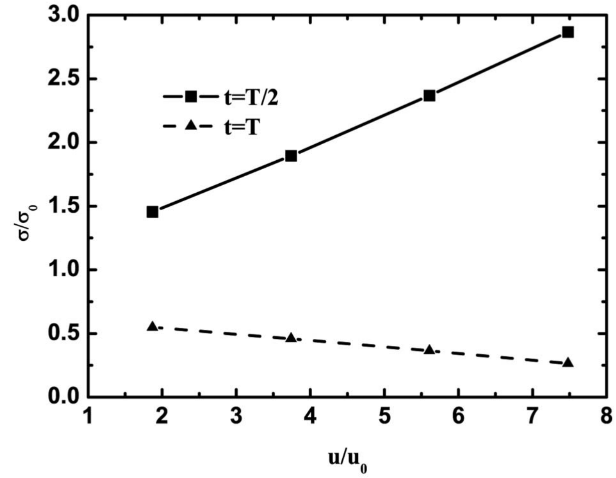

Figure 6. The near-wall shear stress at the lower boundary at $T/2$ and T for different rolling velocities. The maximal relative rolling depth h_{m}/H is 0.6 and the rolling protuberance length L_{s} is 300.

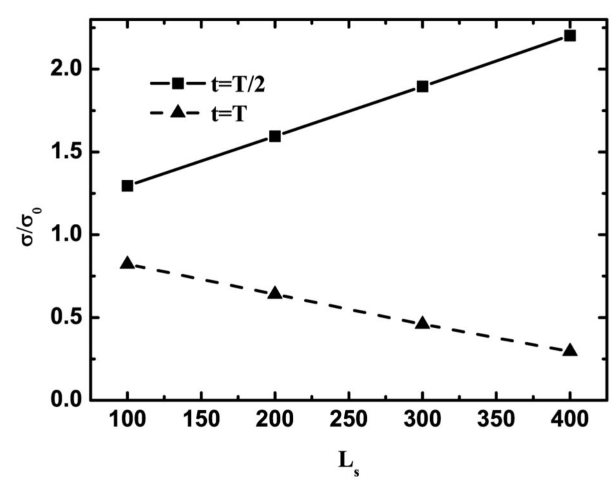

Figure 7. The near-wall shear stress at the lower boundary at $T/2$ and T for different rolling protuberance lengths. The maximal relative rolling depth h_{m}/H is 0.6 and the rolling velocity is 3.74.

However, at entrance and exit of the bend, the enhancement of the near-wall shear stress is negligible; another massage technique is needed in order to remove the blood stasis.

3.2. *The blood flows in the bending artery for different massage technique factors*

The rolling massage technique factors, including rolling velocity, rolling force, rolling moving direction and rolling massage duration, play an important role in massage therapy. Figures 6 and 7 show the relative shear stress σ/σ_0 at $x/H = 225$ near the lower wall at $T/2$ and T for different rolling velocities u/u_0 and rolling protuberance lengths L_s, respectively. σ is the shear stress with rolling massage and σ_0 is the shear stress at the same site in the case of without rolling massage. The near-wall shear stress at $T/2$ increases, as the rolling velocity (protuberance length) increases almost linearly. However, larger rolling velocity (protuberance length) results in the smaller near-wall shear stress at T. Similar results for the near-wall shear stress at other positions in the bending parts can be obtained. The increase and the decrease of near-wall shear stress periodically may be helpful in removing blood stasis.

4. Conclusions

In summary, we used a LBM to study the dynamics of the blood flows in the bending arteries under the rolling manipulation. It is found that the rolling massage technique factors, which are rolling velocity and rolling length, affect the haemodynamics greatly. Our study would be helpful in the understanding of the mechanics of massage in improving blood circulation and removing the stasis. However, the effects of the massage would be very complex, i.e. the blood flow in bifurcations as well as the transportation of the red blood cells and special treatment skills on each acupuncture point. In our future work, we will focus on the effect of the CMM on fluid flows in three dimensions and the effect of massage on these blood flows in a complex blood artery together with the professional therapist.

Acknowledgements

This work was supported by the Natural Science Foundation of Shandong Province of China under Grant Nos. ZR2011AM001, ZR2009AL001 and ZR2009AQ011 and the Scientific Research Foundation of Binzhou University under Grant No. 2007Y03.

References

Artoli, A.M., *et al.*, 2004. Lattice BGK simulations of flow in a symmetric bifurcation. *Future Generation Computer Systems*, 20 (6), 909–916.

Benzi, R., Succi, S., and Vergassola, M., 1992. The lattice Boltzmann equation: theory and applications. *Physics Reports*, 222 (3), 145–197.

Boyd, J. and Buick, J.M., 2007. Comparison of Newtonian and non-Newtonian flows in a two-dimensional carotid artery model using the lattice Boltzmann method. *Physics in Medicine and Biology*, 52 (20), 6215–6228.

Boyd, J., *et al.*, 2004. Application of the lattice Boltzmann method to arterial flow simulation: investigation of boundary conditions for complex arterial geometries. *Australasian Physical and Engineering Science in Medicine*, 27 (4), 207–212.

Boyd, J., *et al.*, 2005. Application of the lattice Boltzmann model to simulated stenosis growth in a two dimensional carotid artery. *Physics in Medicine and Biology*, 50 (20), 4783–4796.

Boyd, J., Buick, J.M., and Green, S., 2007. Analysis of the Casson and Carreau-Yasuda non-Newtonian blood models in steady and oscillatory flows using the lattice Boltzmann method. *Physics of Fluids*, 19, 093103.

Chen, S.Y. and Doolen, G.D., 1998. Lattice Boltzmann method for fluid flows. *Annual Review of Fluid Mechanics*, 30, 329–364.

Chen, H., Chen, S., and Matthaeus, W.H., 1992. Recovery of the Navier–Stokes equations using a lattice gas Boltzmann method. *Physical Review A*, 45 (8), R5339–R5342.

Dupin, M.M., Halliday, I., and Care, C.M., 2003. Multicomponent lattice Boltzmann equation for mesoscale blood flow. *Journal of Physics A*, 36 (31), 8517–8534.

Dupin, M.M., *et al.*, 2008. Lattice Boltzmann modelling of blood cell dynamics. *International Journal of Computational Fluid Dynamics*, 22 (7), 481–492.

Fang, H.P., *et al.*, 2002. Lattice Boltzmann method for simulating the viscous flow in large distensible blood vessels. *Physical Review E*, 65, 051905.

Fung, Y.C., 1997. *Biomechanics circulation*. Berlin: Springer-Verlag.

Hoekstra, A.G., *et al.*, 2003. Lattice BGK simulations of unsteady flow in a 2D elastic tube. *Lecture Notes in Computer Science*, 2657, 997–1006.

Inamuro, T., Maeba, K., and Ogino, F., 2000. Flow between parallel walls containing the lines of neutrally buoyant circular cylinders. *International Journal of Multiphase Flow*, 26 (12), 1981–2004.

Ji, Y.P., Kang, X.Y., and Liu, D.H., 2009. The blood flow at arterial bifurcations simulated by the lattice Boltzmann method. *Chinese Physics Letters*, 26 (7), 074702.

Ji, Y.P., Kang, X.Y., and Liu, D.H., 2010. Simulation of non-Newtonian blood flow by lattice Boltzmann method. *Chinese Physics Letters*, 27 (9), 094701.

Kang, X.Y., *et al.*, 2008. Three-dimensional lattice Boltzmann method for simulating blood flow in aortic arch. *Chinese Physics B*, 17 (3), 1041–1049.

Krafczyk, M., *et al.*, 1998. Simulation and visualization of transient 3D-flow in arteries with an artificial heart valve using lattice-Boltzmann methods. *Journal of Biomechanics*, 31, 453–462.

Li, H.B., *et al.*, 2004a. Lattice Boltzmann simulation on particle suspensions in symmetric severely stenotic arteries. *Physical Review E*, 69, 031919.

Li, H.B., *et al.*, 2004b. Force evaluations in lattice Boltzmann simulations with moving boundaries in two dimensions. *Physical Review E*, 70, 026701.

Li, H.B., *et al.*, 2008. Shape changes and motion of a vesicle in a fluid using a lattice Boltzmann model. *Europhysics Letters*, 81 (5), 54002.

Maria, M., 1997. *The handbook of Chinese massage: tui na techniques to awaken body and mind*. Rochester, VT: Healing Art Press.

McDonald, D.A., 1974. *Blood flow in arteries*. London: Arnold.

Migliorini, C., *et al.*, 2002. Red blood cells augment leukocyte rolling in a virtual blood vessel. *Biophysical Journal*, 83, 1834–1841.

Qian, Y.H., d'Humiéres, D., and Lallemand, P., 1992. Lattice BGK models for Navier–Stokes equation. *Europhysics Letters*, 17 (6), 479–484.

Sun, C.H., Migliorini, C., and Munn, L.L., 2003. Red blood cells initiate leukocyte rolling in postcapillary expansions: a lattice Boltzmann analysis. *Biophysical Journal*, 85, 208–222.

Yi, H.H., 2010. Effect of rolling massage on the vortex flow in blood vessels with lattice Boltzmann simulation. *International Journal of Modern Physics C*, 21 (11), 1421–1431.

Yi, H.H., *et al*., 2005. Lattice Boltzmann simulation of blood flow in blood vessels with the rolling massage. *Chinese Physics Letters*, 22 (12), 3210–3213.

Zou, Q. and He, X., 1997. On pressure and velocity boundary conditions for the lattice Boltzmann BGK model. *Physics of Fluids*, 9, 1591–1598.